MISSOURI S&T

Missouri University of Science and Technology

Scholars' Mine

International Conferences on Recent Advances in Geotechnical Earthquake Engineering and Soil Dynamics

2010 - Fifth International Conference on Recent Advances in Geotechnical Earthquake Engineering and Soil Dynamics

26 May 2010, 4:45 pm - 6:45 pm

Vibrodriving Prediction Models vs. Experimental Results

Valérie Whenham
Belgium Building Research Institute (BBRI), Belgium

Alain Holeyman
Catholic University of Louvain-La-Neuve (UCL), Belgium

Follow this and additional works at: https://scholarsmine.mst.edu/icrageesd

Part of the Geotechnical Engineering Commons

Fifth International Conference on
Recent Advances in Geotechnical Earthquake Engineering and Soil Dynamics
and Symposium in Honor of Professor I.M. Idriss
May 24-29, 2010 • San Diego, California

VIBRODRIVING PREDICTION MODELS VS. EXPERIMENTAL RESULTS

Valérie Whenham
Belgium Building Research Institute (BBRI)
Bruxelles, Belgium 1000

Alain Holeyman
Catholic University of Louvain-La-Neuve (UCL)
Louvain-La-Neuve, Belgium 1348

ABSTRACT

This paper reviews and discusses methods currently available to assess the vibro-driveability of piles based on a comparison between calculations and experimental observations. The experimental results come from databases collected in Belgium and in The Netherlands, as well as from full scale tests campaigns conducted in Belgium and in France. Discrepancies between modeling assumptions and actual observations are highlighted, and some suggestions are made to improve the performance of design methods.

INTRODUCTION

Vibratory driving is based on degradation and liquefaction of the soil around a vibrated profile. The efficiency of the technique depends upon numerous parameters such as the pile to be driven, the selected vibrating equipment and the encountered soil conditions. Its major limitation is a lack of guidelines in relation to driving refusal.

Over the years different engineering design tools and more fundamental modeling approaches have been suggested to assess the vibratory driveability of piles and sheet piles. Models purely based on force equilibrium have been suggested e.g. by [Jonker, 1987], [Azzouzi, 2003], [van Baars, 2004]. These models aim at predicting whether a vibrator can or cannot overcome an estimated soil resistance; they will not provide an estimate of the driving speed. Such an estimate requires that movement be described from inertial equilibrium conditions. The simplest way to analyze the motion of a vibro-drived pile is to consider it as a rigid body mass. Soil resistance is modeled by mathematical expressions, which are based on experimental results and justified from a soil mechanics point of view. Examples of this approach may be seen in [Holeyman, 1993], [Dierssen, 1994], [Vanden Berghe, 2001] and [Sieffert, 2006]. A few researchers have used the finite element method to simulate pile vibrodriving [Chow and Smith, 1984], [Smith and To, 1988], [Leonards et al., 1995], [Graβe et al., 2006], [Cudmani and Sturm, 2006], [Mahutka and Graβe, 2006]. Although finite element results can be used for the development of simpler mechanical models, this approach is too complex and time consuming and therefore inappropriate to solve daily practical problems.

Because of the difficulty to accurately represent the mechanisms at play, vibro-driving prediction methods need to be validated on the basis of experimental observations, preferably by means of fully instrumented real scale driving tests. Such tests have been recently performed in France ([Arnould et al., 2005], [Sieffert, 2004]) and in Belgium ([Whenham et al., 2006], Whenham et al., 2009]). Measurements obtained typically include levels of driving energy, driving frequency and amplitude, vibratory and static forces applied to the sheet pile and penetration velocities.

Experience databases also provide useful information to analyze the performance of design tools on a larger scale. Within the framework of the HiperVib research program [BBRI, 1994] results from 19 sites located in Belgium have been compiled with penetration velocity records. More recently, the Dutch Association of Contractors in Foundation Engineering (NVAF) together with Deltares (former GeoDelft) has developed an on-line database (named GeoBrain) containing about 300 field cases of sheet pile vibrodriving experiences [Hemmen & Bles, 2005].

The present paper first reviews existing tools for pile and sheet pile vibrodriving predictions. An overview of experience databases and full-scale tests measurements is then given, followed by a confrontation between calculation results and actual observations. Some suggestions are finally made to improve the quality of vibro-driving predictions.

COMMON MODELS ASSUMPTIONS

The mechanical action of a vibrator onto a profile consists of two parts: a vibratory action produced by counter-rotating eccentric masses actuated within the vibrating part of the vibrator and a stationary action induced from gravity forces. The net quasi-stationary action on soil is the weight of the pile mass, vibrator mass and clamping device, possibly deduced by the suspension force exerted by the crane operator.

$$F_s = M_{tot}.g - T \tag{1}$$

With F_s = Quasi-stationnary force [kN], M_{tot} = Total mass [T], T = Suspension force [kN]. The amplitude of the vibratory action resulting from the centrifugal forces of the symmetrically moving eccentric masses is given by

$$F_v(t) = me.\omega^2 \sin(\omega t) = F_c \sin(\omega t) \tag{2}$$

With me = Eccentric moment of the vibrator [kg.m], ω = angular frequency of the vibrator [rad/s], F_c = Dynamic force amplitude of the vibrator [kN]. Under the additional assumption that the pile behaves as a rigid body rigidly connected to the exciter block and neglecting the movement of the quasi-stationary mass, the vibrating force leads to a displacement amplitude of the free system

$$d_0 = me / M_{dyn} \tag{3}$$

With M_{dyn} = Total vibrating mass (incl. pile, clamps and vibrator) [T]. Assumptions related to the soil behavior vary significantly from one method to another. In addition to the soil resistance, attention should be paid to the clutch resistance which can be combined with the skin friction.

METHODS ASSESSING VIBRO-DRIVING

Models assessing the vibro-driveability of profiles are reviewed below. Distinction is made between (1) Methods based on force equilibrium, (2) Methods based on a single degree of freedom model and (3) Methods based on a radial soil representation.

Force equilibrium models

Force equilibrium models are the simplest design tools to predict which vibrator is necessary to install a sheet pile without problems.

β-method [Jonker, 1987]. The model calculates for each penetration depth the static and dynamic soil resistance, the remaining amplitude at the pile toe and the acceleration at the toe. The model deduces from these values the so-called beta parameter defined as the ratio between the dynamic and static forces. The obtained beta parameter is compared with limit values deduced from experience in different types of soil. If the parameter is lower than the limit value, the model considers that the vibrator is able to drive the pile into the soil at the considered depth. Apart from being a function of the usual soil parameters, the β values are different for low frequency and high frequency hammers, for open and closed-piles, and may differ for piling and extraction operations. The β values depend further on the acceleration of the pile and may depend on the amplitude of motion also [Jonker and van der Zouw, 2002]. Typical values range from 0.1 to 0.4.

CUR 166 [CUR166, 2005]. Two refusal depth criteria have been published in the dutch CUR-166 manual. They take the form:

$$m.e \geq M_{dyn}.d_{min} \; with \; d_{min} = 0.005m \tag{4a}$$

$$F_c \geq 1,92.10^{-3}.Z_d.\chi.q_{c;z;av} + 1,2.\Omega.q_{c,z,av} \tag{4b}$$

With Z_d = pile penetration height [m], χ = pile perimeter [m], Ω = pile section [m²], $q_{c,z,av}$ = averaged cone resistance value [kPa]. The first relationship states that the displacement amplitude deduced from [equ.3] should be larger than 5 mm in order to overcome soil resistance. The second and complementary equation has been calibrated on calculations made for several standard cases [Azzouzi, 2003] with the computer model Hipervib-I [Holeyman, 1993a]. The method has been further verified on the basis of 18 field tests with varying sheet piles, vibrators and soil conditions. Based on a similar approach, Van Baars (2004) proposed the following equation:

$$F_c \geq \gamma \left(Z_d \Omega \beta \exp(q_{c,tip} / q_{c,ref}) + Z_d \chi \alpha q_{c,tip} \right) \tag{5}$$

With γ = 1.20 [-], α = 0.001 [-], β = 220 [kN/m³], $q_{c,ref}$ = 8700 [kPa], $q_{c,tip}$ = cone resistance at tip of the pile [kPa]. Applicability of this equation is however limited to sites characterized by low cone penetration resistance profiles.

Single degree of freedom models

In the single degree of freedom methods, the vibro-driver-pile-soil system is modeled by a one-dimensional mechanical model with one degree of freedom. The simplification is only valid if the driving frequency is much lower than the vertical resonant frequencies of the pile, since only then the pile behaves approximately as a rigid body. The pile is supposed to be rigidly fastened to the vibrating mass through the clamp. The additional mass is supposed not to interfere with the dynamic movement and has only a static action. The general equation of the pile motion is expressed by:

$$M_{dyn} Acc = F_c \sin(\omega t - \varphi) - F_{toe} - F_{shaft}$$

With Acc = Pile acceleration [m/s²], φ = Phase delay between force & acceleration [rad], F_{toe}, F_{shaft} = Limit values of soil toe & lateral resistances [kN]. The phase constant φ between force and acceleration is not a priori known, while the force and power actually transferred to the pile depend on its value (see [Vié, 2002]).

Hipervib-I [Holeyman, 1993a]. In the Hipervib-I model, the mean speed velocity results from equilibrium between the upward and downward phases of pile motion. This equilibrium can be summarized by two adimensional coefficients:

$K_1=1/(g.M_{dyn})\,[F_c-F_s-(1+\theta).F_{shaft}]$ (Upward motion)
$K_2=1/(g.M_{dyn})\,[F_c+F_s-(1+\theta).F_{shaft}-F_{toe}]$ (Downward motion)

With $\theta = 0.1$ is an adimensional damping coefficient. If K1<0, the penetration speed is nihil: the total driving force (F_c+F_s) cannot overcome the soil resistance. If K1>0, the penetration speed is calculated according to:

$$V_{moy} = K_0\,(K_1{}^2-K_2{}^2).(V_{dyn}-V_{corr}) \qquad (6)$$
$$V_{dyn} = [F_c+F_s-(1+\theta).F_{shaft}-F_{toe}]/(M_{dyn}.\omega)$$

K_0 is a constant equal to 0.0015 and V_{corr} depends on the liquefied value of the mean shaft friction stress:

$$V_{corr} = \sqrt{\frac{F_{shaft}}{Z_d.\chi.\rho.\Gamma}}$$

Where Γ is a constant is equal to 150 and ρ is the soil density [T/m³]. The soil driving resistance is obtained by interpolation between a static value and an ultimately degraded value. The static base (q_s) and shaft (τ_s) resistance profiles derived from Cone Penetration (CPT) tests results. The ultimately liquefied base (q_l) and shaft (τ_l) unit soil resistances are derived based on an exponential law as expressed below :

$$q_l=q_s\left[(1-1/\Lambda)\cdot e^{-3/FR}+1/\Lambda\right] \qquad (7a)$$
$$\tau_l=\tau_s\left[(1-1/\Lambda)\cdot e^{-3/FR}+1/\Lambda\right] \qquad (7b)$$

With FR [%] the friction ratio as measured in a CPT test and Λ an empirical liquefaction factor expressing the loss of resistance attributable to liquefaction (Λ will be higher for saturated and loose sands and is chosen in the range of 4 to 10).

The driving base (q_d) and shaft (τ_d) unit resistances are derived from the static and the "liquefied" soil resistance depending on the vibration amplitude following an exponential law as expressed below:

$$q_d=(q_s-q_l)\cdot e^{-acc/g}+q_l \qquad (8a)$$
$$\tau_d=(\tau_s-\tau_l)\cdot e^{-acc/g}+\tau_l \qquad (8b)$$

Other authors ([Dierssen, 1994], [Gonin, 1998], [Sieffert, 2006]) have proposed methods based on a single degree of freedom system. The main limitation of those studies is a lack of validation and guidelines in relation to soil parameters.

Dierssen [Dierssen, 1994]. The author developed a mechanical model to investigate the driveability of piles in granular soils. The soil resistance at the pile toe considers different phases depending on the pile toe position relative to the soil. As shown in Fig.1., cavitation phase is introduced when the pile toe is not touching the soil.
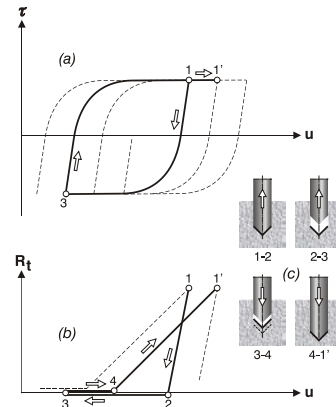

Fig. 1. Resistance mobilization versus displacement for (a) skin (b) toe compression (After Dierssen, 1994)

Gonin [Gonin, 1998]. The author proposed a method that analytically integrates the effects of an excess force, as shown in Fig. 2. The integration is performed solely on the toe resistance, while the skin friction influence is accounted for in terms of damping of the driving force. In addition, the wave equation theory is used to estimate the displacement accrued at the toe over the period of net force exceedance.
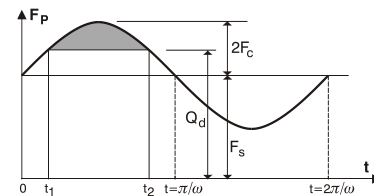

Fig. 2. Integration of excess toe force (after Gonin, 1998)

Vié [Vié, 2002]. For predicting the refusal depth, Vié has proposed a graphical representation in $\zeta=F_{toe}/F_c$, $\psi=F_{shaft}/F_c$ plane, divided in three zones using $\alpha=F_s/F_c$ as a reference parameter (Fig.3):

- Zone (1): no motion at all
- Zone (2): no upward motion

- Zone (3): alternatively upward and downward motion or no motion

According to this diagram, the upward motion will not be possible if $F_s+F_{shaft}>F_c$ (or $\psi>1-\alpha$), while the forces applied on the pile never exceed the soil resistance if $F_{toe}+F_{shaft} > F_s+F_c$ (or $\zeta+\psi>\alpha+1$). However, if an upward motion is possible, a downward motion may occur, at first without contact between pile toe and the soil and then after contact because of the velocity continuity. The possibility of driving while applied forces never exceed soil resistance must be related to the assumption of a loss of contact at the pile toe during upward motions. For $F_{shaft} <F_c-F_s$ (or $\psi<1-\alpha$), the motion is possible independently of the toe resistance, but the mean velocity decreases rapidly as the toe resistance increases.
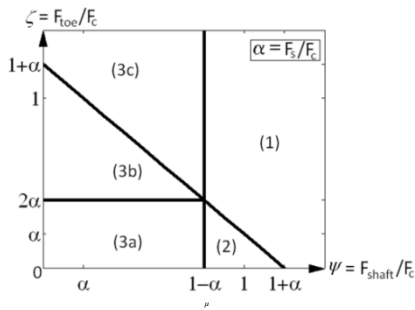

Fig. 3: Vibro-driving domain (after [Vié, 2002]).

Braxuus [Sieffert, 2006]. The Braxuus model calculates the pile displacement during the vibratory driving by integrating the equation of motion. The model considers the pile as a rigid body and calculates the soil resistance assuming a perfect (visco-)plastic behavior. The shaft resistance is directly mobilized in the opposite direction of the pile displacement whereas the toe resistance is directly mobilized only when the pile penetrates deeper than the maximum depth reached during the previous cycles.

Wave propagation models

In the wave equation methods, the pile is divided in a series of elements that are interconnected with springs which stiffness depends on the pile characteristics. The first element represents the static mass and is connected by a soft spring, whereas the second element simulates the exciter block and is subjected to a sinusoidal force. The soil resistance results from non-linear springs and viscous dashpots at toe and the shaft. The penetration rate is obtained by numerical integration of the one-dimensional wave propagation equation. Most of the available models [Rausche, 2002] are based on the assumption that the soil resistances during impact and vibratory driving are similar. However, the penetration mode during vibratory driving strongly depends on the machine parameters and the soil state, and can be rather different from that during impact driving [Cudmani et al., 2002].

Cudmani et al. [Cudmani et al., 2002]. Soil resistance results from non-linear springs and viscous dashpots at toe and the shaft. The energy dissipation due to wave radiation is modeled through velocity dependent forces at the toe and at the shaft. According to [Dierssen, 1994] model, the soil resistance at the pile toe considers different phases depending on the pile toe position relative to the soil and a cavitation phase is introduced when the pile toe is not touching the soil. The parameters of the model are estimated from impact penetration and vibro-penetration tests.

Radial 1-D models

Holeyman [Holeyman, 1993b] has suggested the use of a radial discrete model to calculate the vertical shear waves propagating away from the pile. The geometric shape of the soil model surrounding the pile has cylindrical symmetry. It is a disk with a thickness that slightly increases linearly with the radius to simulate the geometrical damping provided by the half-space of soil located below the toe of the pile. The soil is represented by discretizing the medium into concentric rings that have their own individual mass and transmit forces to their neighbours. The movement of the sheet-pile and the rings is calculated from the time integration of the law of motion: the equations of movement are integrated for each cylinder based on their dynamic shear equilibrium in the vertical direction. An energy absorbing boundary condition in accordance with plane-strain elasticity theory [Novak et al., 1978] limits the lateral extent of the model at a distance large enough to ensure that deformations stay within the elastic range and to avoid artificial energy reflections.
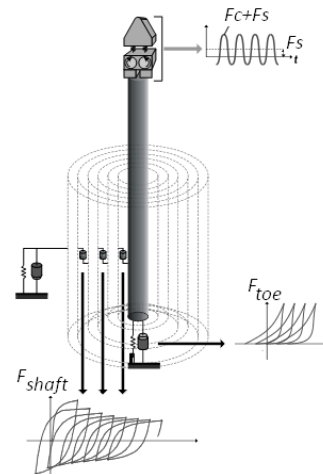

Fig. 4. Radial model [after Holeyman, 2000]

Hipervib-II [Holeyman, 1993b]. The model makes use of constitutive relationships representing the large-strain, dynamic and cyclic shear stress-strain strength, behavior of the medium surrounding the vibrating profile. To evaluate the shear force-displacement relationship between successive rings, the model applies:

- Hyperbolic law [Kondner, 1963] to describe the static behavior of soil where η = Mobilization ratio [-], τ_{max} = Ultimate shear stress [kPa] and G_{max} = Initial (tangent) shear modulus [kPa]. Values of τ_{max} and G_{max} are based on correlations with data obtained from CPT (FR is the friction ratio [%] and f_s is the local skin friction [kPa]).

$$\eta = \frac{\tau}{\tau_{max}} = \frac{\gamma.G_{max}/\tau_{max}}{\gamma.G_{max}/\tau_{max}+1}$$
$$G_{max} = 15.q_c$$
$$\tau_{max} = \beta.f_s = \left[0,65 + 0,35.\tanh(1,5.(FR-2\%))\right]f_s$$

- Masing's laws [Masing, 1926] to represent the hysteresis, where $f(\tau,\gamma)=0$ and (τ_c,γ_c) is the point of maximum straining.

$$f\left(\frac{\tau_c+\tau}{2};\frac{\gamma_c+\gamma}{2}\right)=0 \ and \ f\left(\frac{\tau_c-\tau}{2};\frac{\gamma_c-\gamma}{2}\right)=0$$

- The strain rate effect is represented by the following power law:

$$\tau_{dynamic} = \tau_{static}.(1+J.\dot{\gamma}^n)$$

Where $\dot{\gamma}^n$ = strain rate and J,n = viscous parameters which depend on the nature of the soil. Based on pile driving data, n=0.2 and J=0.1*FR s$^{-0.2}$ have been adopted.

- When subjected to undrained cyclic loading involving a number N of large strain cycles, the soil structure continuously deteriorates, the pore pressure increases, and the secant shear modulus decreases. This behavior is taken into account thanks to the following equations:

$$\tau_N = \Delta.\tau_{N=1} = N^{-t}.\tau_{N=1} \ and \ G_s = \Delta.G_{max}.(1-\eta)^2$$
$$t = \frac{\sqrt{\gamma/\gamma_{tu}-1}}{PI/2+25}, \ \gamma_{tu}=\beta.FR/30 \tag{9}$$
$$PI = 50(1+\tanh(FR-3.5\%))$$

The Δ coefficient expresses the degradation from the static value resulting from the cyclic nature of loading. The exponent t, called degradation parameter, depends mainly on the amplitude of the cyclic strain and the nature of the material (plasticity index PI), as suggested by [Dobry and Vucetic, 1987] and [Vucetic, 1994]. The degradation parameter assumes a zero value at strains smaller than a cyclic "threshold" shear strain, γ_{cv} The threshold strain increases with the plasticity of the soil.

Vipere [Vanden Berghe, 2001]. The soil behavior is assumed to be hypoplastic and modeled using the [Bauer, 1996] and [Gudehus, 1996] constitutive law. The model considers the behavior of the soil is undrained with each soil element being simply sheared. In order to calculate the toe resistance of the pile during the vibratory driving, the VIPERE model represents the soil under the pile by a cylinder. The soil at the

pile base and the pile are supposed to stay permanently in contact. The soil behavior of the soil cylinder at the pile toe is assumed to be hypoplastic and the element is supposed to be loaded in triaxial conditions. One rare feature of the VIPERE model is its ability to follow pore pressure variations through the various states experienced by the soil during the cycles as a result of dilatant or contractive phases of the behavior of the soil skeleton. With this model, the three-dimensional character of the volume change trends can be accommodated respectively in a pure shear for the skin friction along the shaft as well as in compression under the pile toe. Practical use of the model is however limited by the need to identify the 8 parameters of the hypoplastic model, although promotors of the hypoplastic model continuously propose new correlations with more usual soil properties (in particular with grain size properties).

EXPERIMENTAL RESULTS

Databases provide a tremendous advantage in regrouping a large number of experiences under various soil and driving equipment conditions. Amount of information related to each case is however generally quite limited. On the other hand, full-scale driving tests with extensive measurements are necessary to better understand the process underlying the vibratory technique, and to verify and calibrate theoretical models. In addition to the penetration velocity, monitoring in full scale tests consists of three parts: the vibratory equipment (eg. energy developed by the power pack, position of the eccentric masses, frequency), the profile (eg. vibration frequency and amplitude, load and power actually transferred from the vibrator towards the soil) and the soil (eg. soil particle velocity).

The study presented in this paper makes use of experimental results collected within the following frameworks.

HiperVib research programme [BBRI, 1994]

The Hipervib research programme featured 28 vibro-driveability case studies at 19 different sites in Belgium, including Hingene, Kortrijk and Limelette. For each case, penetration velocity profile and refusal depth have been reported. For some cases, signals from accelerometers and strain gauges positioned on the sheet pile are also available.

GeoBrain database [Hemmen and Bles, 2005]

The GeoBrain experiences database contains case histories for foundation and drilling technology. Since 2005, contractors have been feeding this database with their experiences in the Netherlands. Today (2009), more than 400 entries are related to the vibratory installation of piles and sheet piles. An experience is defined by the type of element, the type of

equipment used and the soil conditions. For the sake of the present paper, 52 case histories have been selected based on following criteria: (1) completeness and reliability of the reported experience, (2) homogeneous soil conditions.

<u>Limelette full scale tests (2003-2007)</u>

A series of tests have been conducted on the test site of Limelette (Belgium) between 2003 and 2007, where instrumented sheet piles have been installed and continuously monitored. Parameters of these tests are described in Table 1. The soil conditions at the test site consist of a medium to stiff silty layer underlaid by compact sand (see Fig. 5). The groundwater table lies approximately 60m below ground level.
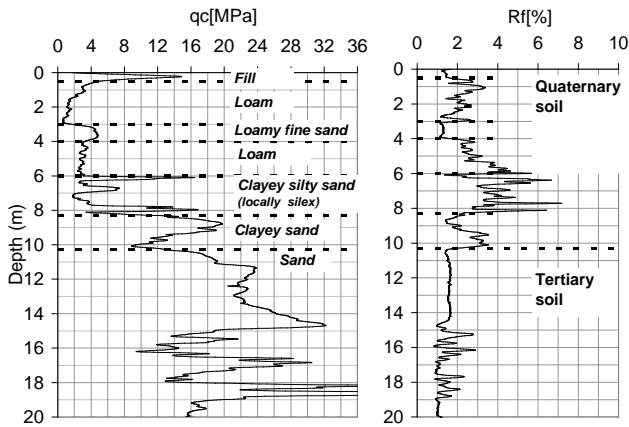

Fig. 5. CPT-E results – Test site of Limelette.

Table 1. sheet piles & vibratory parameters – Limelette site

Profile	Pile I	Pile II	Pile III	Pile IV	Pile V	Pile VI
Perimeter [m]	4.14	4.14	4.48	3.30	3.30	3.30
Section [m²]	0.0311	0.0305	0.0302	0.0199	0.0199	0.0199
Length [m]	20	22	22	20	20	20
Dyn.mass (excl.pile) [kg]	5100	5100	5100	5770	5770	5770
Nominal me [kg.m]	35	35	35	36	36	36
Nominal Frequency [Hz]	33.3	31.8	32.4	32.8	22	37.7
Refusal depth [m]*	6.75	6.75	7.25	Not reached **	6.70	Not reached **

    * Penetration speed < 0.1m/min
    ** Pile driving was intentionally stopped at 7m

<u>Merville full scale tests [Arnould et al. 2006, Sieffert 2004]</u>

The tests have been conducted within the framework of a research project organized in France between November 2000 and December 2005. LCPC and INSA of Strasbourg have carried out most of the data processing related to the experiments of that project [see Sieffert 2004]. Different types of sheet piles were driven in Flanders clay, along with an open tube. General information about the tests is summarized in Table 2. Geotechnical parameters are presented in Table 3.

Table 2. Merville test site [Sieffert 2004]

Profile	Open Tube	Sheet pile 1	Sheet pile 2	Sheet pile 3	Sheet Pile 4
Perimeter [cm]	160	440	440	838	330
Section [cm²]	266	230	230	590	190
Length [m]	12.3	13	16	11	16
Dynamic mass (excl.pile) [kg]	4910	5660	5660	5660	5660
Nominal me [kg.m]	46	46	46	46	46
Nominal Frequ. [Hz]	26	26	26	26	26
Refusal depth [m]*	5.5	6	6...6.5	6...6.5	5.5..6.5

    * Penetration speed < 0.1 m/min

Table 3. Merville geotechnical data [Sieffert, 2004]

Depth [m]	Nature	P_l^* [MPa]	E_M [MPa]	q_c [MPa]
0 to 2.2m (at 1m)	Loam	0.25	3.7	0.7
2.2 to 42m (at 4m) (at 16m)	Flanders clay	0.75 1.8	14 35	2 5

    P_l^* = Menard limit pressure, E_M = Menard E-modulus
    q_c = cone resistance

MODEL ASSUMPTIONS VS. MEASUREMENTS

In this section, commonly adopted model assumptions regarding force and displacement amplitudes are criticized in light of experimental measurements (see also [Whenham & Holeyman 2008]).

<u>Force exerted on the pile</u>

The force actually transmitted to the pile is only a fraction of the vibratory action developed by the vibrator. This fraction depends on the vibrator-pile mass ratio (M_v/M_p) and on the pile-soil system boundary conditions. As an example, forces deduced from strain gauges measurements obtained at the Limelette test site are presented in Fig. 6, along with theoretical values obtained (a) assuming that the vibrator action is totally transmitted to the pile and (b) taking into account a load transfer correction factor $f(K_T)$ defined by [eq.10] and obtained from wave propagation considerations.

$$f(K_T) = \left(1 + \frac{M_v}{M_p} \cdot \frac{\omega^2 . M_p - \alpha . tg(\alpha) . K_T}{K_T + \omega^2 . M_p . \alpha^{-1} . tg(\alpha)}\right)^{-1} \qquad (10)$$

where $\alpha = \omega . L/c$, L is the pile length and c is the pile wave velocity. That correction factor is the solution of the wave equation assuming that: (1) the vibrator behaves as a rigid body, (2) the pile behaves as an axially elastic body connected at the toe to a spring characterized by a stiffness coefficient K_T [N/m]. The value of the K_T stiffness coefficient has been back-calculated based on displacement amplitudes measured at different levels on the sheet pile, as shown in figure 7. It can be noted that the toe displacement amplitude is larger than that at the head of the sheet pile.

(a)

(b)
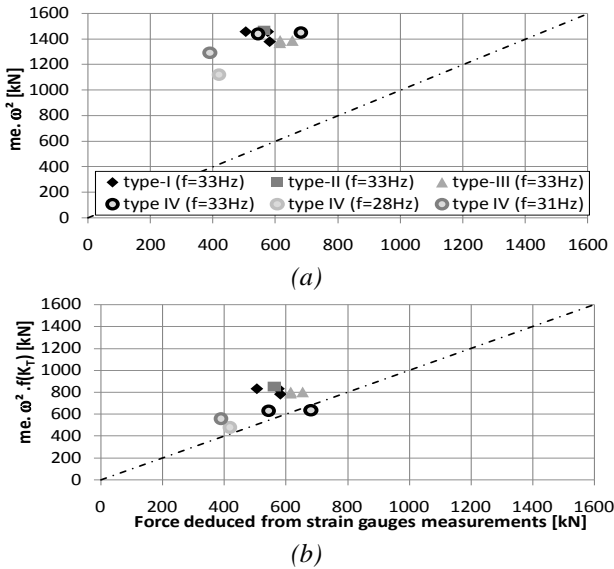
Fig. 6 (a) Force transferred from the vibrator to the pile
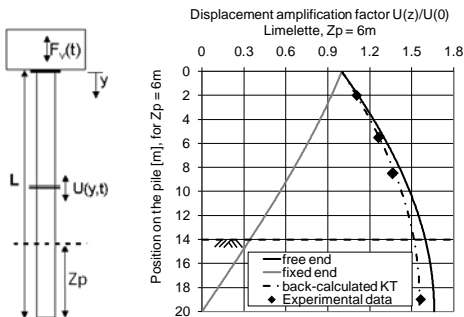
Fig. 7. (a) Force transferred from the vibrator to the pile and (b) Back-calculation of K_T value based on monitored displacement profile at Limelette (Zp = 6m)

Discrepancy between nominal and actual vibratory action can also be caused by a power demand (required to overcome soil resistance) that exceeds the maximal capacity of the power pack. This will result in a decrease in the driving frequency, as illustrated in Fig. 8 (see [Holeyman & Whenham 2008]).
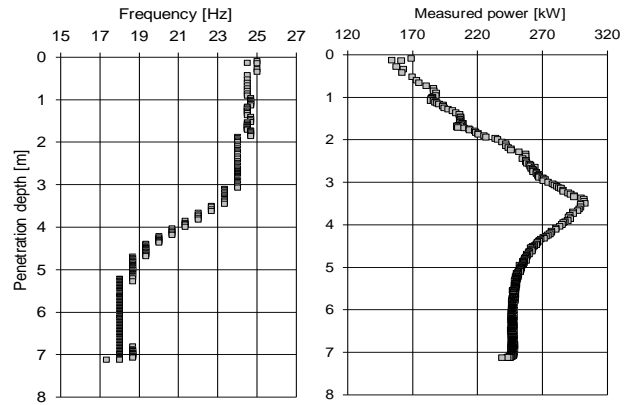

Fig. 8. Evolution of (a) dominant frequencies, (b) power developed by the power pack – in function of the penetration depth (Merville, Flanders clay) [Sieffert, 2004]

Displacement amplitude

Discrepancies between free (nominal) displacement amplitudes [equ.3] and actual displacement amplitudes can be attributed to pile elasticity and soil boundary conditions effects. Assuming the power pack is adequately designed and the dynamic mass is correctly estimated, displacement amplitudes measured at the top of the sheet pile agree generally quite well with [equ.3], as shown in Fig. 9(a). Displacement amplitudes measured at the pile toe may however be much lower for that case than at the pile top, as depicted in Fig.9(b).
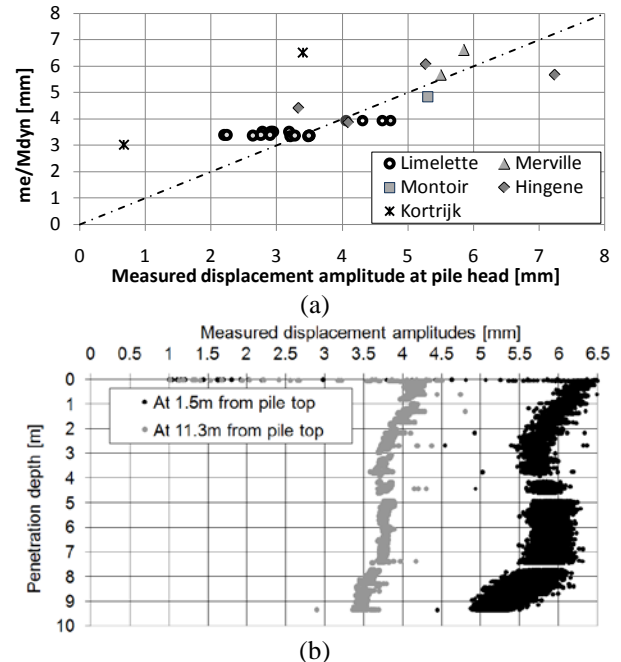

(a)

(b)

Fig.9. Displacement amplitudes (a) at the top of sheet piles (Hipervib database & Limelette tests), (b) on an open tube (Merville, Flanders clay), at 1.5m and 11.3m from the pile top.

REFUSAL DEPTH

The aim of this section is to give a global overview of refusal depth criteria's from various driving prediction tools as compared to experimental observations. Three design models have been selected, respectively based on the CUR-166 rules and on the Hipervib-I and Hipervib-II models. Motivation for this choice is that all three approaches only require basic information concerning driving equipment (usual parameters) and soil properties (CPT results). Depending on the method, one or two criteria are required; either based on force equilibrium or on imposed minimal displacement/velocity amplitude. Criteria are applied assuming that the driving force and displacement amplitude are defined by [equ.2] and [equ.3], except for the Limelette tests where a correction factor could be applied, based on the back-calculated load factor $f(K_T)$. Experimental results from databases have been classified according to soil conditions: "Base resistance" sites are characterized by a high cone resistance and a low friction ratio, "Friction resistance" sites are characterized by a high friction ratio and a low cone resistance, and "other" sites are characterized by relatively high friction and cone resistances. Cases histories for which some "problems" to reach the desired depth have been reported are differentiated from "success" cases stories. Parameters adopted to describe the Limelette full scale driving tests correspond to situations where refusal depths were not reached (with penetration velocities $v_p = 0.5$m/min), whereas parameters of the Merville tests correspond to refusal depths.

CUR 166. The CUR 166 method considers two refusal depth criteria: a first one based on equilibrium between driving and resisting force and a second one based on a minimal displacement amplitude of 5mm. Both criteria are applied to the GeoBrain and Hipervib databases (Fig. 10 & 11), as well as to the results from the Limelette and Merville test campaigns (Fig. 12 & 13).
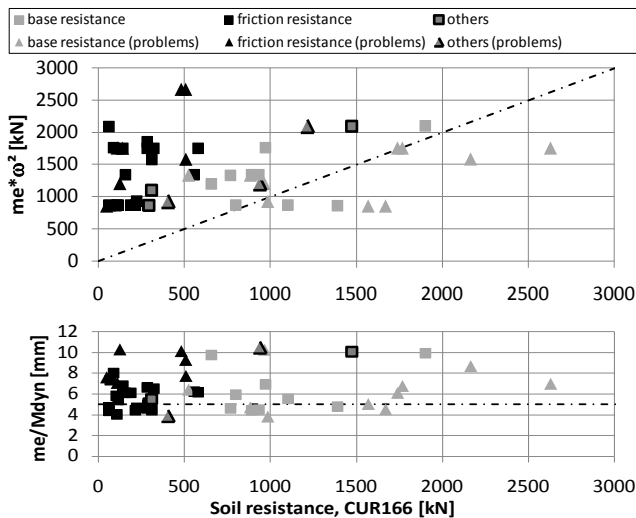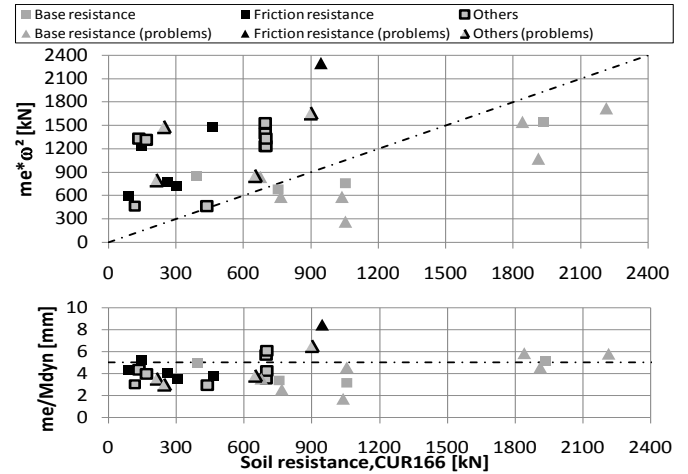

Fig.11. CUR 166 criteria applied to the Hipervib database

When applying the CUR166 equation, soil resistances calculated for cohesive soils ("friction resistance") are systematically lower than soil resistances calculated for granular soils ("base resistance"). This can be explained by the fact that [equ.4a] is only based on cone penetration resistance results, without consideration for the friction ratio values. Soil cyclic degradation is however much more pronounced in granular soils. Underestimation of the soil resistance in cohesive soils is evidenced by comparing CUR166 criteria and Merville (site characterized by overconsolidated Flanders clay) tests results (Fig. 12a). Also the displacement amplitude criteria do not include influence of the friction ratio. No distinction is made between cohesive and granular soils neither in the required displacement amplitude nor in the estimation of the displacement amplitude. Contrary to experimental observations, the minimum displacement amplitude criterion is respected for the Merville tests but not for the Limelette tests (Fig. 12 and 13).
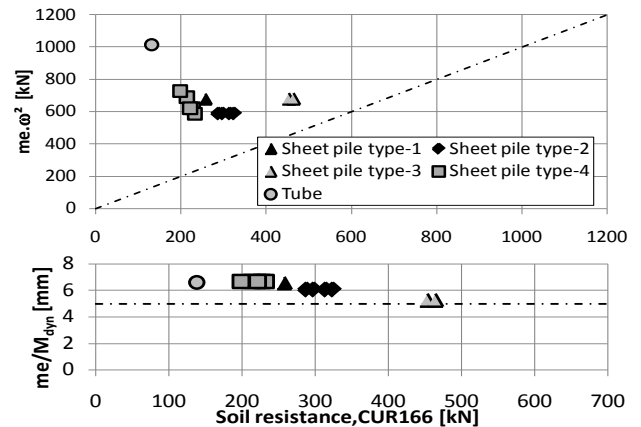

Fig. 12. CUR 166 criteria applied to Merville tests (at refusal depth, Zp = 5.5-6.5m)
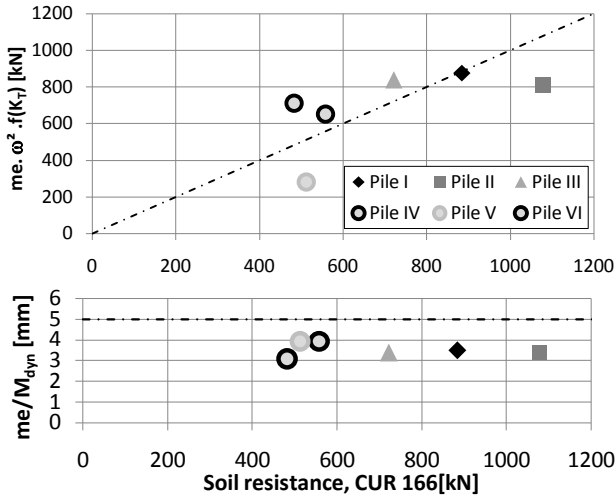

Fig. 10. CUR 166 criteria applied to the GeoBrain database

Fig. 13. CUR 166 criteria applied to Limelette tests (at refusal depth: Zp=6.70m - except for piles IV and VI: Zp=6.70m).

It can be further observed that the water level is not included in [equ.4], while saturation of the soil is a key factor in soil cyclic degradation.

Hipervib-I. This method is also based on two criteria. The first one can be expressed by comparing the driving force with the soil degradated resistance. The second one is a velocity amplitude criterion [see equ.6]:

$$V_{dyn} = \frac{F_c + F_s - (1+\theta).F_{shaft} - F_{toe}}{M_{dyn}.\omega} > V_{corr} = \sqrt{\frac{F_{shaft}}{Z_d.\chi.\rho.\Gamma}}$$

Application of the Hipervib-I refusal depth criteria to experimental data from the GeoBrain and Hipervib databases and from the Merville and Limelette tests campaigns are respectively shown in Fig. 14 to 17.
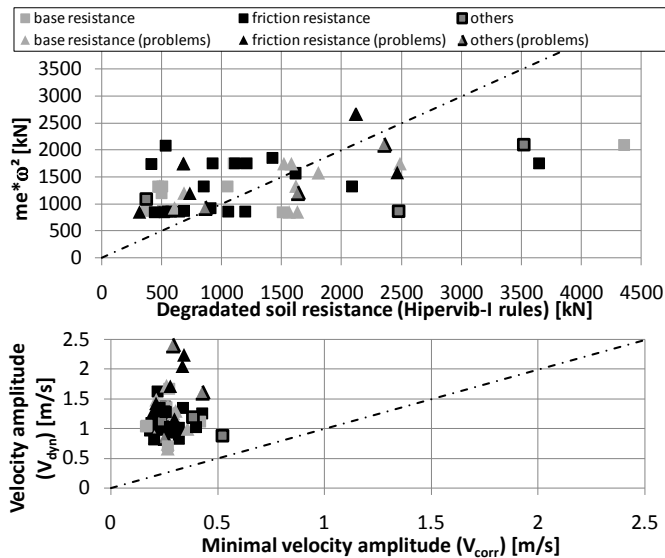

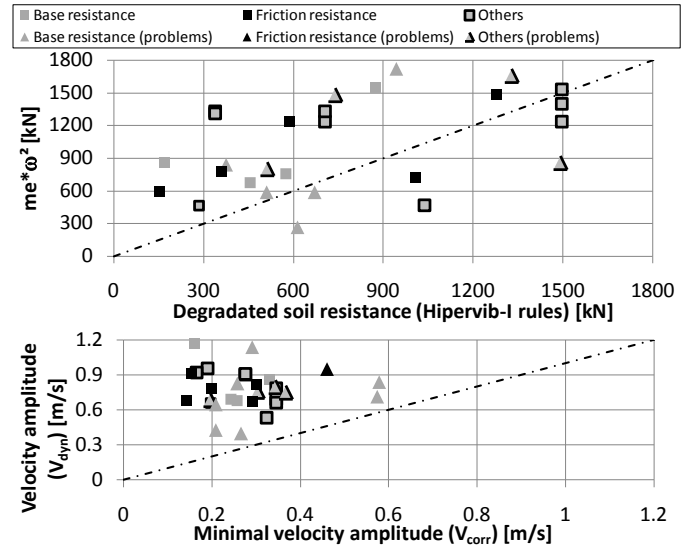Fig. 14. Hipervib-I criteria applied to the GeoBrain database

Fig. 15. Hipervib-I criteria applied to the Hipervib database

The friction ratio is included in the soil resistance definitions, in particular in the degradation laws. Soil cyclic degradation is also function of the driving amplitude, while the soil saturation can be taken into account by adapting the choice of soil degradation parameters [equ.7]. By comparing Fig. 10-11 to Fig. 14-15, it can be observed that soil resistances calculated according to the Hipervib-I model ([equ. 7-8]) are generally higher than soil resistances obtained according to CUR166 rules. The shaft resistance influences the velocity amplitude criterion as well as the evaluation of the velocity amplitude.
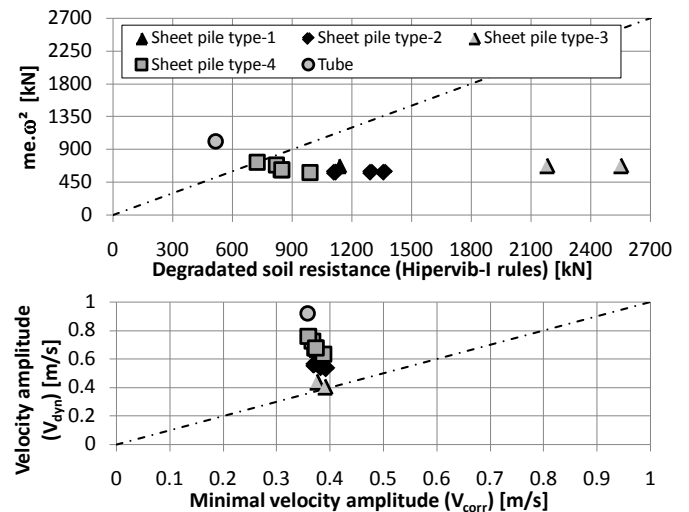

Fig. 16. Hipervib-I criteria applied to the Merville data (at refusal depths)

To take into account the effect of pile elasticity in the velocity amplitude criteria applied to the Limelette data, [equ.6] has been corrected as follows:

$$V_{dyn,K_T} = V_{dyn}.f^*(K_T) = V_{dyn}.\frac{M_v + M_p}{\left(M_v + M_p.\dfrac{K_T + \omega^2.M_p.\alpha^{-1}.tg(\alpha)}{\omega^2.M_p - \alpha.tg(\alpha).K_T}\right)}$$

Results presented in Fig. 17 are too pessimistic as compared to experimental data. A reason can be the application of the $f(K_T)$ correction factor, while the method has been calibrated based on the [equ.2] assumption. A closer look at results indicates however that the calculated soil resistances are mainly (almost only) due to shaft friction, also when the pile penetrates the compact sand layer, which is not realistic (at Limelette, refusal has only be encountered when the pile reached the compact sand layer, due to base resistance). That can be due to the fact that similar degradation laws are adopted for shaft and base soil degradation, while the shaft resistance is probably more degradated under cyclic loading than the base resistance. That can also be explained by the fact that neither "friction fatigue" nor lateral vibrations effect are accounted for. Both phenomena can be expected to influence (decrease) the shaft resistance at a large distance from the tip, especially for long piles.
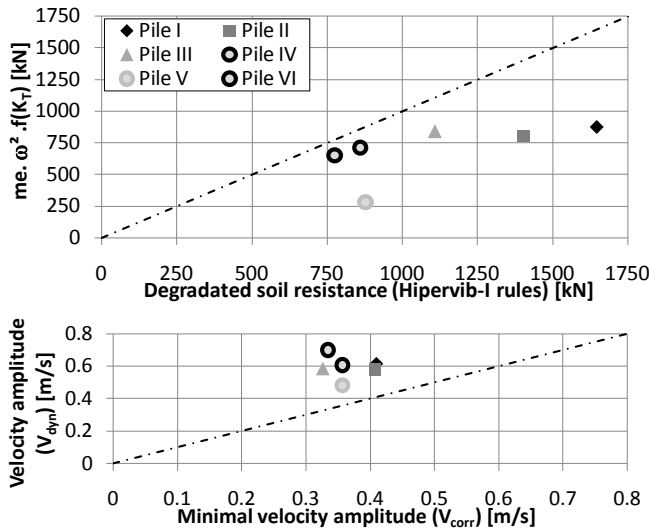

Fig. 17. Hipervib-I criteria applied to the Limelette data (at refusal depth except for piles IV and VI).

Hipervib-II. To study the refusal depth criteria implicitly implemented in the Hipervib-II method, integrals of soil resistance has to be compared to integrals of driven force. To facilitate the interpretation, comparison is expressed below in terms of RMS values. No explicit displacement amplitude criterion is defined in this method, although a minimum shear strain is required to achieve soil degradation according to [equ.9].
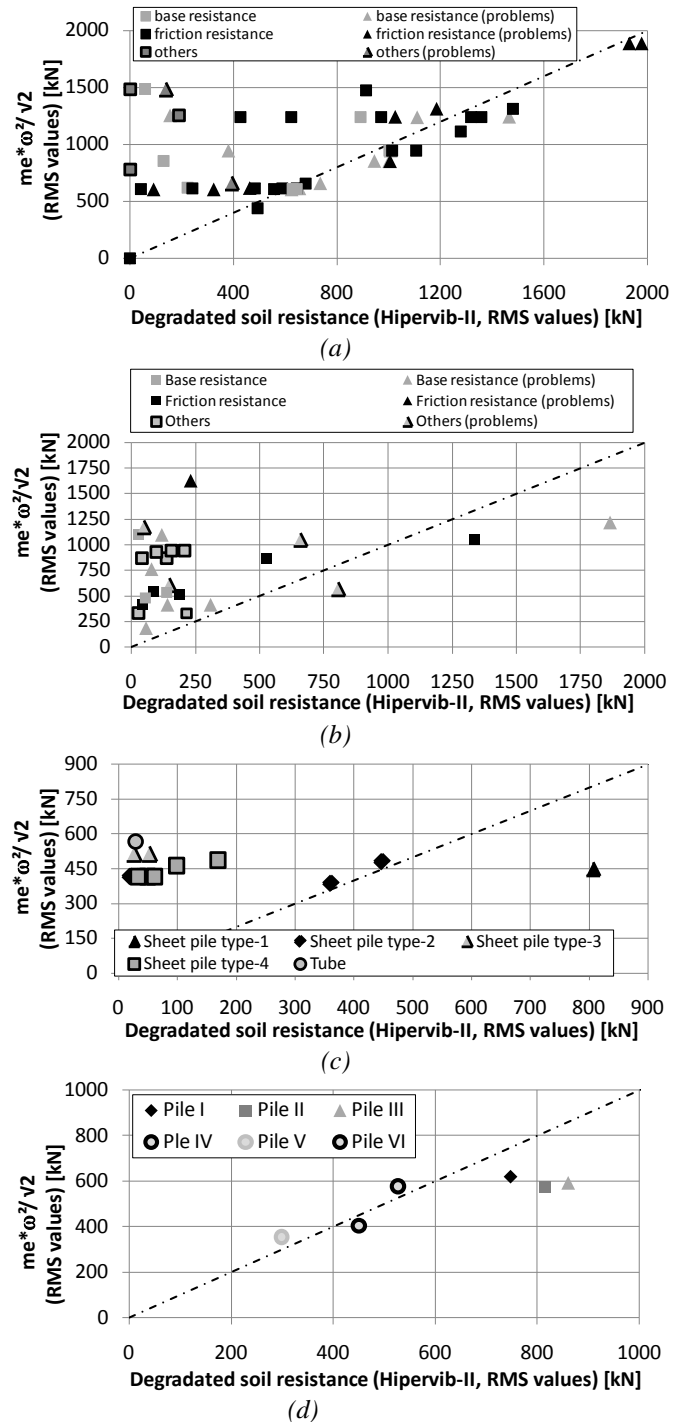

Fig. 18. Hipervib-II applied to the (a) the GeoBrain database, (b) the HiperVib database, (c) Merville results (refusal depth), (d) Limelette results (refusal depth exc. piles IV & VI).

The Hipervib-II model leads to lower soil resistances as compared to the CUR166 and Hipervib-I methods. Applied to the Merville results, the method gives too optimistic results.

PENETRATION VELOCITY

With Hipervib-I and Hipervib-II methods, pile penetration velocity can also be obtained. In Fig. 19, penetration velocities calculated with Hipervib-I and Hipervib-II are compared with penetration actually measured at the Merville test site. As previously observed based on the study on refusal depths, the Hipervib-I method gives very satisfactory results while the Hipervib-II method overestimates penetration velocities.
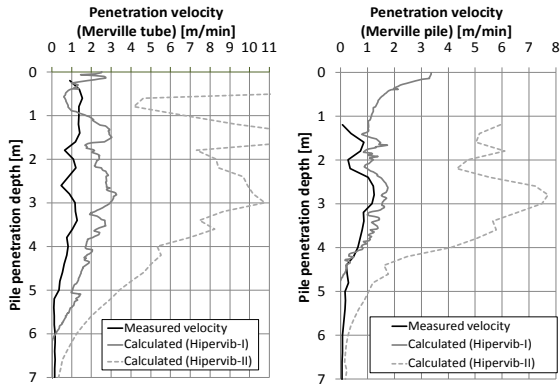

Fig. 19. Penetration velocity profiles for the sheet pile n°1 and the open-tube driven at the Merville site (Flanders clay)

Penetration velocities highly depend on the static force applied to the pile [equ.1], as illustrated in Fig. 20. Assuming that the applied force is harmonic, it can be shown that driving is only possible when $F_{toe} < 2.F_s$ (see [Holeyman, 1993], [Gonin, 1998]) i.e. $\zeta < 2.\alpha$ (cfr Fig.3.). The difference in the minimum static force required is therefore due to the difference in calculated base resistances.
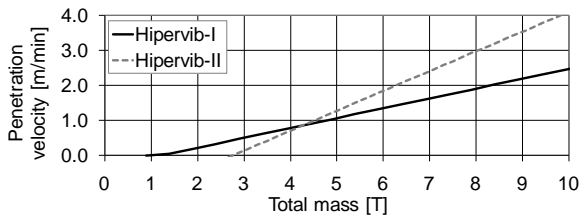

Fig.20. Influence of the static force on the penetration velocity

Figure 21 depicts the influence of the driving velocity amplitude on sheet pile penetration velocity: (1) as experimentally deduced from tests performed at the Limelette test site with various frequencies and amplitudes [Whenham et al., 2009], (2) as calculated using respectively the Hipervib-I and Hipervib-II method. Distinction is made between increases in velocity amplitudes due to varying frequencies or eccentric moments. The minimal velocity criterion as well as the global evolution of penetration velocities are reasonably well reproduced by Hipervib-I. Using Hipervib-II, the influence of the driving frequency is much more pronounced.
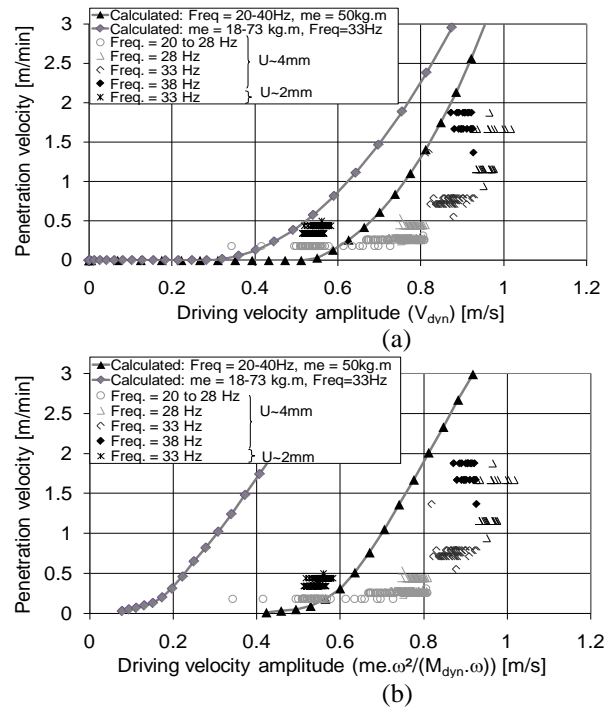

(a)

(b)

Fig. 21. Penetration velocity vs. (nominal) acceleration amplitude as calculated with (a) Hipervib-I, (b) Hipervib-II

CONCLUSIONS

The aim of this paper was to review some vibro-driving prediction tools in comparison to experimental data issued from databases and full scale sheet pile vibro-driving tests. Main conclusions are the followings.

(1) Assumptions usually adopted in vibro-driving models contrast with experimental evidence and can lead to significant consequences for the driveability prediction of the profile. Discrepancy mainly concerns the vibratory action (load and energy) actually transmitted to the pile.

(2) Some methods consider two criteria: one based on a force equilibrium between active and resisting forces, the other based on mínimum displacement amplitudes. Combination of these two criteria lead to a better estimation of refusal depth.

(3) The friction ratio deduced from CPT results has to be taken into account in soil degradation calculation and displacement amplitude criterion definition.

(4) Differentiation between soil degradation laws for shaft and base resistances should prevent a systematic overestimation of shaft resistance as compared to base resistance.

(5) The application of a particular model for driveability predictions depends on conditions of validation of the model. Accurate procedure for the estimation of the model parameters is also essential.

REFERENCES

Arnould P., Canou J., Gonin H., Guillaume D., Keller P., Legendre Y., Legrand ., Rocher-Lacoste F., Sieffert J-G, Vié D. [2005]. "Guide Technique du Vibrofonçage 2005", *Projet National Vibrofonçage 2000-2005*

Azzouzi S. [2003]. "Intrillen van stalen damwanden in niet-cohesieve gronden", *GeoDelft NL &. TU. Delft NL.*

Barkan, D. [1963]. "Méthodes de vibration dans la construction", *Dunod, Paris, 302 p.*

BBRI [1994]. "High performance vibratory pile drivers base on novel electromagnetic actuation systems and improved understanding of soil dynamics", *Progress reports of the BRITE/EURAM research contract CT91-0561, 1994.*

CUR 166 [2005]. "Damwandconstructies", *Civieltechnisch Centrum Uitvoering Research en Regelgeving (NL)*

Cudmani R., Huber G.,Gudehus G. [2002] "A mechanical model for the investigation of the vibrodriveability of piles in cohesionless soils". *Proc. Int. Conf. on Vibratory Pile Driving and Deep Soil Compaction, Transvib2002, LLN, 53-60.*

Dobry, R. and Vucetic, M. [1987]. "State-of-the-Art Report: Dynamic Properties and Response of Soft Clay Deposits". *Int. Symp. on Geot. Eng. of Soft Soils, Mexico, Vol. 2, pp. 51-87.*

Gonin, J. [1998] "Quelques réflexions sur le vibrofonçage", *Revue Française de Géotechnique N°83, 2e trimestre, pp35-39*

Hemmen, B.R & Bles, T [2005]. "GeoBrain Funderingstechniek: Ervaringsdatabase voorspelt uitvoeringsrisico". *Civiele Techniek, 60 (2005) 2, pp.24-25*

Holeyman, A. [1993a] "HYPERVIB1, An analytical model-based computer program to evaluate the penetration speed of vibratory driven sheet Piles", *Research report for BBRI, 23p.*

Holeyman, A. [1993b] "HYPERVIBIIa, A detailed numerical model proposed for Future Computer Implementation to evaluate the penetration speed of vibratory driven sheet Piles", *Research report for BBRI, 54p.*

Holeyman, A. & Legrand, C. [1994]. "Soil Modelling for pile vibratory driving", *Int. Conf. on Design and Construction of Deep Foundations, Vol.2, pp1165-1178,Orlando,U.S.A.,1994.*

Holeyman, A. [2000]. "Vibratory Driving Analysis – Keynote Lecture". *VIth Int. Conf. on the Application of Stress-Wave Theory to Piles, Sept. 11, 12 & 13, 2000, Sao Paulo, Brazil.*

Holeyman, A. & Whenham, V. [2008]. "Sheet pile vibro-driving: Power pack-vibrator-sheet pile-soil interactions". *Int. Conf. on the Appl.of Stress Wave Theory to Piles, Lisbon 2008*

Idriss, I.M., Dobry, R, and Singh. R.D. [1978]. "Nonlinear Behavior of Soft Clays during Cyclic Loading." *J. Geotechnical Eng. Div., ASCE, 104(GT12), pp. 1427- 1447.*

Jonker G. [1987]. "Vibratory Pile Driving Hammers for Oil Installation and Soil Improvement Projects". *Proc.19th Annual Offshore Technology Conf., Dallas, Texas, pp.549-560.*

Kondner, R. L., [1963]. "Hyperbolic Stress-Strain Response: Cohesive Soils." *Journal of the Soil Mechanics and Foundations Division, ASCE, Vol. 89, No. SM1, pp.115-143.*

Masing, G. [1926], "Eigenspannungen und Verfeistigung beim Messing", *Proc.2nd Int. Congress of Appl.Mech., pp. 332-335.*

Novak M., Nogami T., Aboul-Ella F. [1978]. "Dynamic Soil Reactions for Plane Strain Case", *J. Engrg. Mech. Div., ASCE, 104(4), 953-959.*

Rausche F. [2002] "Modeling of vibratory pile driving". *Transvib2002, LLN, 21-32.*

Sieffert J.-G. [2002] "Vibratory pile driving analysis. A simplified model". *Transvib2002, LLN, 53-60.*

Sieffert J.-G. [2004] "Essais de Merville. Interprétation et modélisation" *Research report IREX LC/03/VBR/29, 127pp.*

van Baars S. [2004]."Design of sheet pile installation by vibration". *Geotech. and Geol. Eng., Vol.22, Nb.3/ Sept. 2004.*

Vanden Berghe, J-F, [2001] "Sand Strength degradation within the framework of pile vibratory driving", *doctoral thesis, Unversité catholique de Louvain, Belgium, 360pages.*

Vié, D. [2002] "Simple model for prediction of vibratory driving and experimental data analysis of vibro-driven probes and sheet piles". *TransVib 2006, Paris, Sept.21-22, 2006*

Vucetic, M. [1994]. "Cyclic Threshold Shear Strains of Sands and Clays", *ASCE Journal of Geotechnical Engineering*

Whenham, V., Huybrechts, N., Legrand, C., Bourdouxhe, M-P. And Schmitt, A. [2006]. "Energy consumption during sheet piles vibro-driving: experimental results". *TransVib 2006, Paris, France, September 21-22, 2006*

Whenham, V. & Holeyman, A. [2008]. "Sheet pile vibro-driving: Assumptions vs. measurements". *Int. Conf. on the Application of Stress-Wave Theory to Piles, Lisbon (2008)*

Whenham V., Areias L., Rocher-Lacoste F., Vie D., Bourdouxhe M-P., Holeyman A. [2009]. "Full scale sheet pile vibro-driving". *Proc. of the 17th Int. Conf. on Soil Mechanics & Geotech. Eng. Alexandria, Egypt 5-9 Oct. 2009.*